THE JOURNAL OF PHYSICAL CHEMISTRY A
A JOURNAL OF THE AMERICAN CHEMICAL SOCIETY

pubs.acs.org/JPCA

Article

Theoretical Assessment of Carbon Dioxide Reactivity in Methylpiperidines: A Conformational Investigation

Uttama Mukherjee,* Prabhat Prakash,* and Arun Venkatnathan*

Cite This: *J. Phys. Chem. A* 2023, 127, 3123−3132

Read Online

ACCESS | Metrics & More | Article Recommendations | Supporting Information

ABSTRACT: In this work, the possible mechanisms for the reactions of CO_2 with various positional isomers of methylpiperidines (MPs) (N-MP, 2-MP, 3-MP, and 4-MP) including the effect of aqueous solvation have been explored using quantum chemical methods. The major pathways investigated for CO_2 capture in aqueous amines are carbamate formation, its hydrolysis, and the bicarbonate formation (CO_2 + H_2O + MP) reaction. The calculations indicate that an axial orientation for the methyl group and an equatorial for the COO^- group could be energetically ideal in the carbamate product of MPs. The proton abstraction step in the carbamate pathway is almost barrierless for the zwitterion-amine route, while a much higher energy barrier is observed for the zwitterion-H_2O route. During carbamate hydrolysis, the addition of even two explicit water molecules does not exhibit any notable effect on the already high energy barrier associated with this reaction. This indicates that bicarbonate formation is less likely to occur via carbamate hydrolysis. The calculations suggest that, although the carbamate pathway is kinetically favored, the MP carbamate could still be a minor product, especially for sterically hindered conformations, and the bicarbonate pathway should be predominant in aqueous MPs.

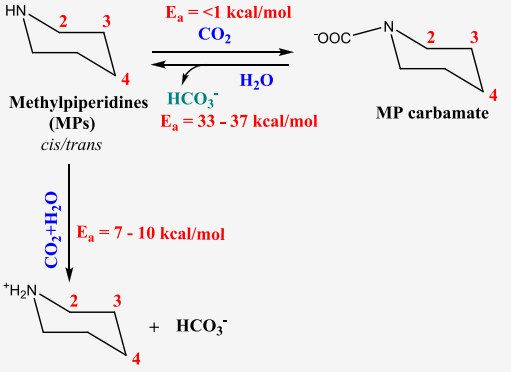

1. INTRODUCTION

Amine-based absorbents are one of the frequently investigated compounds for post-combustion CO_2 capture (PCC). Among various amines, monoethanolamine (MEA) and diethanolamine (DEA) have been used for small-scale industrial operations.[1] The chemical reactions of amines with CO_2 and the formation of various products and pathways are summarized in Scheme 1.[2,3]

In aqueous amines, the chemical absorption of CO_2 leads to a carbamate or bicarbonate product (reactions 1 and 3 in Scheme 1). From previous studies,[4−8] it has been demonstrated that the primary and secondary amines in general form carbamate derivatives upon reacting with CO_2 in an aqueous medium. Carbamate formation is a base-catalyzed nucleophilic reaction that proceeds via a zwitterion intermediate where the second amine molecule acts as the Brønsted base. The carbamate derivative may hydrolyze to produce bicarbonate and regenerate back the free amine (reaction 2, Scheme 1), though less likely as the carbamate species is quite stable in the case of primary and secondary amines. Tertiary amines or other hindered amines do not form a carbamate by directly reacting with CO_2 and rather follow the bicarbonate pathway. Further, it has also been manifested that amines with carbamate as the major product exhibit faster reaction rates (kinetically favorable)[9] but a lower absorption capacity[10] due to a 2:1 amine−CO_2 stoichiometry and also require higher regeneration energies.[11] In contrast, amines with bicarbonate as the major product show kinetically less favored reactions with higher absorption capacities and lower regeneration energies.[12,13] Thus, investigating the relative formation of carbamate versus bicarbonate is essential in comprehending the absorption capacity, rate of absorption, and regeneration properties of aqueous amine solvents for carbon capture.

Quantum chemistry methods, such as density functional theory (DFT), have been routinely used to calculate quantitative thermodynamic properties and propose reaction mechanisms. da Silva and Svendsen[14] studied the stability of carbamates for a series of amines using different solvation models and concluded that carbamate stability of amines is an important factor in determining their chemistry and overall performance as CO_2 absorbents. Jackson et al.[15] performed a full conformational analysis of a series of aqueous amines for CO_2 capture using DFT and MP2 methods. This investigation revealed the poor CO_2 capture performance of NH_3 and sterically hindered amines, such as 2-amino-2-methyl-1-propanol (AMP), while an enhanced one for cyclic amines (piperidine and piperazine). Xie et al.[16] used DFT methods to investigate the reaction mechanism of MEA with CO_2 in aqueous solution. The authors demonstrated that the amine−CO_2 reaction is a two-step

Received: January 18, 2023
Revised: March 6, 2023
Published: March 16, 2023

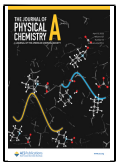

Scheme 1. Major Reactions Involved in CO_2 Capture by Aqueous Amines: (1) Carbamate Formation, (2) Carbamate Hydrolysis, and (3) Bicarbonate Formation[a]

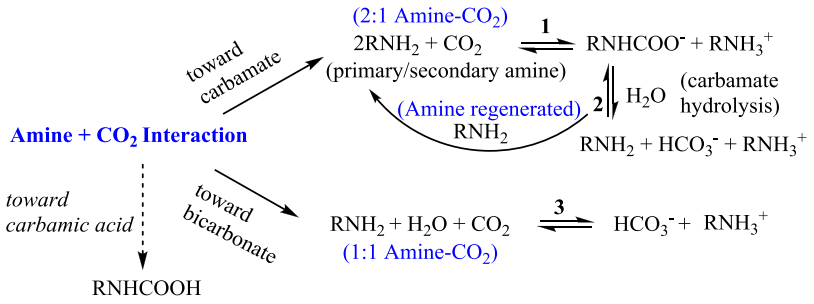

[a]The carbamic acid formation is a possibility under anhydrous conditions. R = H, CH_3, CH_2OH, C_2H_4OH.

process that proceeds through a zwitterion intermediate, and the formation of a zwitterion is the rate-determining step. The authors have further explained that the second step in this reaction involves H-abstraction from the zwitterion, which is almost barrierless. Yamada et al.[17] studied the interaction of CO_2 with moderately hindered amines (such as 2-isopropylaminoethanol) using quantum chemical methods. They predicted that carbamate formation is a kinetically fast reaction while bicarbonate is the major product for moderately hindered amines. Stowe et al.[18] studied the thermodynamic and kinetic factors associated with the CO_2 absorption mechanism in aqueous AMP,[19] a sterically hindered primary amine. The authors observed that AMP's protonation occurs more favorably than carbamate formation in aqueous solutions as AMP is a stronger base. The authors emphasized on the significance of kinetic factors while considering CO_2−aqueous amine reactions. Yamada[20] explored the effect of the dielectric constant of the solvent in aqueous amines and amine-functionalized ionic liquid anions using quantum mechanical calculations. From the study, it was observed that the conventional reaction between CO_2 and amines in a solvated environment largely depends on the dielectric constant of the solvent while amine-functionalized anions easily form stable C−N bonds irrespective of the dielectric constant of the solvent. Said et al.[21] have proposed a general pathway for the CO_2−amine reaction mechanism (aqueous/non-aqueous) based on previous theoretical and experimental works. The authors have concluded that bicarbonate formation begins as the amine concentration decreases (with the CO_2 pressure maintained), and the carbamate, which is initially formed, decomposes back to an amine. In the presence of tertiary amines and sterically hindered amines, H_2O becomes a stronger nucleophile attacking the electrophilic CO_2, and thus, the bicarbonate pathway is followed.

In general, cyclic amines have been found to be more advantageous over other alkanolamines (such as MEA and DEA) for CO_2 absorption as these have high CO_2 absorption capacities and fast absorption rates (first-order reaction) and require lower regeneration energy.[22−27] Piperidine, a heterocyclic secondary amine, is one such example that has been studied as a suitable CO_2 absorbent.[28−31] Piperidine has enhanced solubility in water as compared to other cyclic amines such as piperazine. In addition, piperidine has been found to have high CO_2 absorption rates with a pK_a of 11.22 and withstand oxidative and thermal degradation.[22,32] Among numerous studies discussed above, a detailed thermodynamic and mechanistic approach for each pathway (Scheme 1) of the methylpiperidine (MP)−CO_2 interaction has not been accomplished so far. Thus, in this work, we have performed a full conformational analysis of the positional isomers of MPs, namely, *N*-methyl (N-MP), 2-methyl (2-MP), 3-methyl (3-MP), and 4-methyl (4-MP), reactions of their conjugate acids (protonated amines), non-bonded complexes, transitions states (TSs), and carbamate products formed during the course of carbon capture reactions. Using conventional thermodynamic cycles, the solution-phase free energy (ΔG_{aq}) of each of the reaction pathways has been estimated together with the computation of aqueous phase equilibrium constants, K_{eq}. MP-CO_2 binding energies (BEs) have been calculated (corrected with a basis set superposition error (BSSE)) to estimate the extent of non-bonding interactions in MPs. The activation energy (E_a) barriers for each pathway have been determined in the solution phase to predict the predominant route followed by the MPs for CO_2 capture. The computational details are presented in the following section, and the variation of ΔG_{aq} and E_a of MP conformers for each reaction pathway is discussed in the Results and Discussion. The major outcomes of this work are summarized in the concluding remarks.

2. COMPUTATIONAL DETAILS

A Gaussian 09-Rev.D01[33] software package was used for all the quantum chemical calculations. Geometry optimization for each conformer of all the species including free amines and protonated amines and their carbamates was performed using two different functionals: B3LYP[34] and M06-2X.[35] An empirical Grimme's dispersion correction[36,37] was employed for all the calculations performed using both the functionals. The 6-311++G(d,p) basis set was used for all calculations. The solvent-phase optimizations (with water as the implicit solvent) using the SMD[38] solvation model (solvation model based on density), which utilizes the IEF-PCM[39] (integral-equation formalism polarizable continuum model) approach, were performed to estimate the free energy of solvation (ΔG_{sol}) of various reaction species. Vibrational frequencies were also calculated at the same level ensuring the structures to be a stationary point (reactants, non-bonded complexes, and products) or a TS (with one imaginary frequency). Relaxed potential energy surface (PES) scans of the reacting species for each pathway with the relevant reaction sites (as the scan coordinate) were performed to obtain the starting geometries. The TS structures were validated using QST2[40] with guess reactant−product pairs. The transition states were further confirmed by an IRC[41,42] (intrinsic reaction coordinate) method. We have included both the E_a (activation energy) and $\Delta^{\ddagger}G°$ (free energy of activation) values to compare the results with other works.[21]

https://doi.org/10.1021/acs.jpca.3c00406
J. Phys. Chem. A 2023, 127, 3123−3132

The 2-, 3-, and 4-MPs have four possible stable conformers, namely, *cis*-axial (*cis*-ax), *cis*-equatorial (*cis*-eq), *trans*-axial (*trans*-ax), and *trans*-equatorial (*trans*-eq), whereas piperidine (pip) and N-MP have only axial (ax) and equatorial (eq) conformers (Figure 1). The gas-phase reaction energies (ΔG_g) were calculated for each of the reactions (Scheme 1) initially. This was followed by the calculation of ΔG_{sol} for each of the species. The details of the calculations pertaining to ΔG_{aq}, K_{eq}, and BE of the relevant piperidine species are discussed in the Supporting Information.

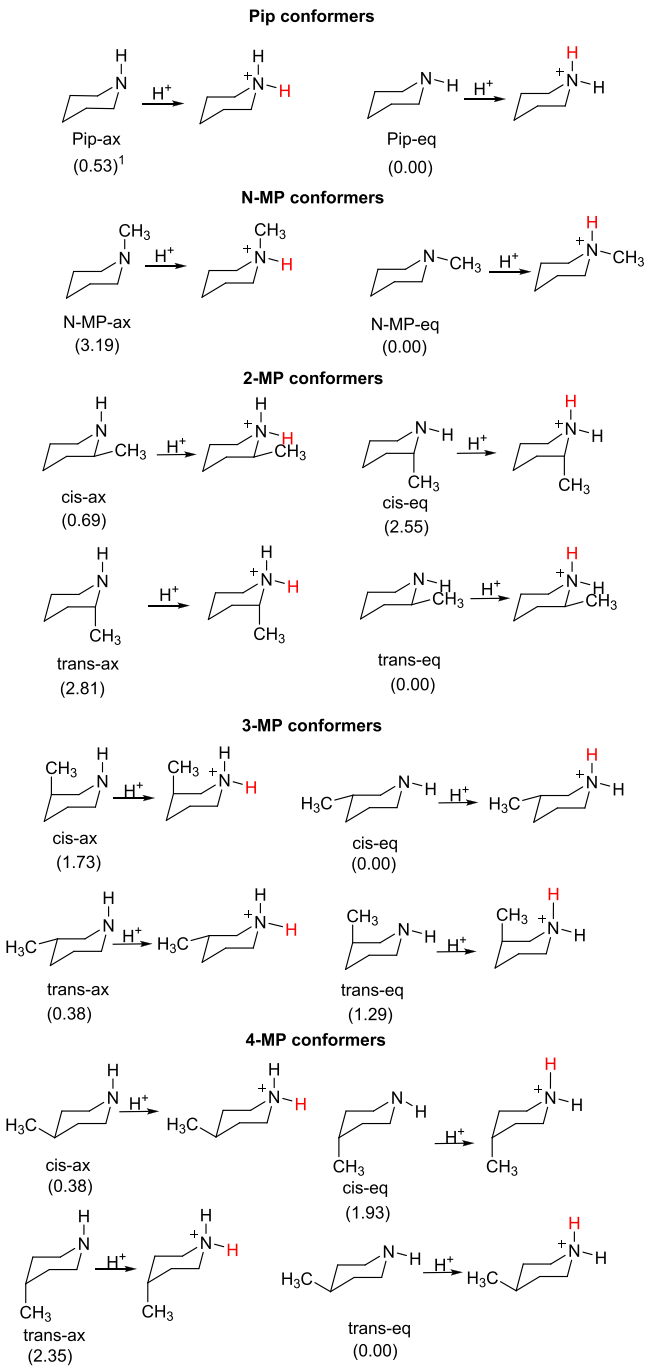

Figure 1. Piperidine (Pip) and methylpiperidine (N/2/3/4-MP) conformers and their protonated forms. Relative energies (kcal/mol) from B3LYP optimized geometries of the conformers (gas phase) are provided in parentheses. [1]The relative energy of pip conformers (gas phase) has been calculated to be 0.55 kcal/mol at B3LYP/6-311G** and 0.53 kcal/mol at MP2/6-311G**.[43]

The relative energies of each conformer in the gas phase and aqueous phase are given in Figure 1 and Table 1, respectively.

Table 1. Relative Energies (kcal/mol) of MP Conformers (Solvent Phase, SMD Model) from B3LYP Optimized Geometries

molecules	conformers			
piperidine	0.00 (ax)		0.36 (eq)[a]	
N-MP	2.71 (ax)		0.00 (eq)	
	cis-ax	*cis*-eq	*trans*-ax	*trans*-eq
2-MP	0.00	2.21	2.03	0.06
3-MP	1.28	0.55	0.00	2.58
4-MP	0.00	2.35	1.82	0.50

[a]The relative energy of pip conformers (solvent phase, PCM) has been calculated to be 0.33 kcal/mol at HF/6-31G* and 0.42 kcal/mol at HF/6-311G**.[43]

The calculated gas-phase relative energies for pip conformers with the B3LYP functional are in excellent agreement with the MP2 level calculations earlier reported in the literature.[43] It is to be emphasized that the stability order (based on relative energies) of pip and MP conformers differ significantly in the gas and aqueous phases. In Figure 1, the gas-phase stability order is provided for better clarity of the functional group orientation. In the aqueous phase, except for N-MP, the stability order of MP conformers (including pip conformers) is observed to be precisely reversed for the *cis*-ax:*trans*-eq and *trans*-ax:*cis*-eq pair. Hence, the aqueous phase stability order will only be considered while discussing the carbon capture reactions in subsequent sections.

The geometrical parameters of eq-pip calculated with B3LYP and M06-2X functionals are compared with the experimental results in Table S1. Although comparable, the geometries optimized with the B3LYP functional show slightly better agreement with the experimental values than M06-2X. Moreover, the calculated rotational constants of eq- and ax-pip as given in Table S2 also agree well with the experimental results. In this case too, the B3LYP functional provides slightly better comparison (for the rotational constants, A, B, and C, and the quartic centrifugal distortion constants, D_J, D_K, and D_{JK}) with experiments compared to M06-2X.

Proton affinities (PAs) and gas-phase basicities (GPBs) for each pip conformer have also been calculated (Table S3) as these aid in predicting the relative basicity of the conformers and are significant for the reactions involving proton exchange equilibria.[15] From the table, it is observed that the values from the M06-2X functional are slightly lower than those of B3LYP. The calculated values for eq-pip and N-MP are close to their experimental values, which indicate that both the functionals are efficient in predicting the PA and GPB of MPs. The basicity trends reveal that the PA and GPB for 2-MP and N-MP are higher than other MPs as the weak electron-donating methyl group is close to the N atom of pip. The PA (and GPB) values of 3-MP and 4-MP are close to each other.

The discussion regarding gas-phase reaction free energies (ΔG_g) and free energies of solvation (ΔG_{sol}) is provided in Tables S4−S6 and S7−S9, respectively. The free energies of solvation of small molecules/ions (H_2O, CO_2, and HCO_3^-)[44−46] involved in the CO_2 capture reaction pathways are provided in Table S10. Further, the $\Delta\Delta G_{sol}$ values of pip and

https://doi.org/10.1021/acs.jpca.3c00406
J. Phys. Chem. A 2023, 127, 3123−3132

MP conformers for all the three capture pathways are provided in Tables S11−S13.

Table 2 shows the solution-phase reaction free energies (ΔG_{aq}) of carbamate formation, carbamate hydrolysis, and bicarbonate formation reactions of pip conformers. From the table, it is observed that most of the ΔG_{aq} values are exoergic except for the carbamate hydrolysis reaction calculated using the M06-2X functional, which is slightly endoergic. Nevertheless, apart from the free-energy parameters for carbamate hydrolysis reaction (ΔG_g, $\Delta\Delta G_{sol}$, and ΔG_{aq}), the B3LYP and M06-2X results follow similar trends. For most of the reactions (Scheme 1), results from B3LYP are closer to the previously calculated values in the literature.[14,15] Thus, we primarily focus on the results obtained from B3LYP. The inclusion of the dispersion correction has a notable effect on the thermochemical data (the reference ΔG_{aq} values[14,15] in Table 2 for eq-pip do not include dispersion effects).[54] Other than ΔG_{aq}, the inclusion of dispersion effects also has a remarkable impact on the ΔG_g corresponding to carbamate hydrolysis as shown in Table S5.

Table 2. Solution-Phase Reaction Free Energies, ΔG_{aq} (kcal/mol), of Reactions 1, 2, and 3 (Scheme 1) for Pip Conformers Using B3LYP and M06-2X Functionals

	B3LYP			M06-2X	
piperidine	ax	eq	calculated values for eq-pip[14,15]	ax	eq
(1) carbamate formation	−4.40	−4.26	$\lesssim -1.00$	−8.52	−4.81
(2) carbamate hydrolysis	−4.95	−4.24	−6.10	3.76	1.61
(3) bicarbonate formation	−8.96	−9.33	~ -6.70	−4.76	−3.21

The discussion regarding aqueous equilibrium constants (K_{eq}) corresponding to reactions 1, 2, and 3 (Scheme 1) and the gas-phase BSSE-corrected interaction energies (ΔE_{int}) of the various MP conformers is provided in Tables S14 and S15, respectively. The K_{eq} results for MP conformers indicate their adequate performance as carbon capture solvents whereby the equilibrium shifts mostly toward the product side. Similarly, the interaction energy results suggest that the ΔE_{int} of MP−CO_2 complexes is at par with the multinitrogen-containing strong bases (such as guanidine, 7-azaindole, imidazole, triazole, etc.), NMe_3, $HCONH_2$, and pyridine as investigated by Lee et al.,[47] which offers one of the reasons as to why MPs have been a material of choice for efficient CO_2 capture. Structures of the 4-MP (conformers)−CO_2 non-bonded complexes optimized with B3LYP and M06-2X functionals showing H-bond distances are provided in Figure S2a,b.

In order to further validate the theoretical results, the optimized geometries of the pip−CO_2 molecular complex (piperidinium-1-piperidinecarboxylate complex) from B3LYP and M06-2X functionals are compared with the experimental geometry determined by Jiang et al.[48] through X-ray single crystal diffraction in Table S16. The optimized structure of the complex with the B3LYP functional is shown in Figure S3. The computed values are in good agreement with the experimental results.

3. RESULTS AND DISCUSSION

3.1. Solution-Phase Reaction Energies. *3.1.1. Carbamate Formation.* The solution-phase reaction energies (ΔG_{aq}) for the carbamate formation reactions of the various conformers of MPs are listed in Table 3. The ΔG_{aq} trends using B3LYP and M06-2X functionals are similar, however, with a significant difference in their magnitudes, especially in the case of *cis*-ax and *trans*-eq conformers of 2-MP. Both conformers do not favor the CO_2 attack due to steric hindrance from the methyl group in proximity. The *cis*-eq 2-MP and *trans*-ax 2-MP (with a methyl group at the axial position) have a lower ΔG_{aq} and are predicted to be the conformers for carbamate formation. This observation is also supported by Tremaine and co-workers,[27,49] who employed experimental and theoretical NMR and IR techniques to confirm the existence and stability of 2-MP carbamate in an aqueous solution. The authors concluded that the major conformer of 2-MP carbamate has a methyl group at the axial position. In the case of 3-MP and 4-MP conformers, *cis*-eq and *trans*-eq 3-MP and *cis*-eq 4-MP indicate a stronger preference for carbamate formation. Overall, ΔG_{aq} data suggest that 3-MP and 4-MP have a slightly higher carbamate formation tendency than unsubstituted piperidine.

Table 3. Solution-Phase Reaction Free Energies, ΔG_{aq} (kcal/mol), Associated with the Carbamate Formation Reaction (See Scheme 1) of MP Conformers from B3LYP and M06-2X Functionals

piperidines	B3LYP	M06-2X
	2-MP	
cis-ax	−0.18	−3.77
cis-eq	−6.48	−9.95
trans-ax	−4.84	−8.68
trans-eq	1.23	−2.22
	3-MP	
cis-ax	−4.21	−9.00
cis-eq	−5.71	−8.16
trans-ax	−4.64	−8.27
trans-eq	−6.44	−9.06
	4-MP	
cis-ax	−4.31	−8.39
cis-eq	−5.92	−8.36
trans-ax	−4.78	−7.82
trans-eq	−4.73	−7.78

3.1.2. Carbamate Hydrolysis. The solution-phase reaction energies for carbamate hydrolysis aid in understanding the relative stability of the various MP carbamate conformers. Table 4 shows the ΔG_{aq} values for the carbamate hydrolysis reaction. The results from the B3LYP functional suggest that the carbamates of *cis*-ax and *trans*-eq conformers of 2-MP show facile hydrolysis as compared to other 2-MP conformers (these conformers showed the least tendency toward carbamate formation as well (Table 2)). The ΔG_{aq} values from the M06-2X functional differ significantly from B3LYP for this reaction (as discussed in the previous section in Table 1). For MPs, the ΔG_{aq} values from the M06-2X functional are endoergic as opposed to exoergic values from B3LYP. da Silva and Svendsen[14] and Jackson et al.[15] reported exoergic ΔG_{aq} values for this reaction in the case of eq-pip using the B3LYP functional. However, the difference in the magnitude of ΔG_{aq} values between conformers are found to be similar in many cases regardless of their absolute values (such as between *cis*-ax and *cis*-eq and *trans*-ax and *trans*-eq conformers) as shown in Table 4 where the ΔG_{aq} values for carbamate hydrolysis of MPs are compared using B3LYP, M06-2X, and ωB97XD functionals.

https://doi.org/10.1021/acs.jpca.3c00406
J. Phys. Chem. A 2023, 127, 3123−3132

Table 4. Solution-Phase Reaction Free Energies, ΔG_{aq} (kcal/mol), Associated with Carbamate Hydrolysis Reaction (See Scheme 1) of MP Conformers from B3LYP, M06-2X, and ωB97XD Functionals

piperidines	B3LYP	M06-2X	ωB97XD
	2-MP		
cis-ax	−10.46	−1.62	−2.80
cis-eq	−5.26	3.77	3.22
trans-ax	−5.51	2.95	1.50
trans-eq	−10.84	−3.14	−4.63
	3-MP		
cis-ax	−6.56	3.92	2.31
cis-eq	−3.76	3.28	3.42
trans-ax	−4.23	3.89	3.31
trans-eq	−3.69	2.98	3.35
	4-MP		
cis-ax	−4.56	3.66	2.62
cis-eq	−3.70	3.10	3.54
trans-ax	−4.42	2.97	3.25
trans-eq	−4.41	2.96	2.57

The calculated values also exhibit only a small difference in ΔG_{aq} for 3-MP and 4-MP conformers.

3.1.3. Bicarbonate Formation. The ΔG_{aq} values in Table 5 show that most of the MPs follow the bicarbonate pathway with

Table 5. Solution-Phase Reaction Free Energies, ΔG_{aq} (kcal/mol), Associated with the Bicarbonate Reaction (See Scheme 1) of Methylpiperidine Conformers Using B3LYP and M06-2X Functionals

piperidines	B3LYP	M06-2X
	N-MP	
ax	−9.44	−4.94
eq	−9.29	−4.39
	2-MP	
cis-ax	−10.04	−5.39
cis-eq	−10.46	−6.18
trans-ax	−10.08	−5.73
trans-eq	−10.07	−5.36
	3-MP	
cis-ax	−8.71	−5.08
cis-eq	−9.47	−4.89
trans-ax	−8.87	−4.38
trans-eq	−10.13	−6.11
	4-MP	
cis-ax	−8.88	−4.73
cis-eq	−9.62	−5.25
trans-ax	−9.20	−4.85
trans-eq	−9.35	−4.82

greater spontaneity. Even the sterically hindered *cis*-ax and *trans*-eq 2-MP favor the bicarbonate pathway. The ΔG_{aq} values calculated using the B3LYP functional are comparatively more exoergic than the M06-2X functional. N-MP, being a tertiary amine, can capture CO_2 only via the bicarbonate pathway as there is no proton on the N atom to initiate carbamate formation. Overall, the ΔG_{aq} values provide a comparative analysis of the conformational preference toward major carbon capture pathways during the aqueous MP−CO_2 interaction.

The dominant pathway leading to carbon capture in each MP and its conformers cannot be predicted solely via ΔG_{aq} data. For this, further study of the reaction pathway and energy barrier for each step needs to be investigated. Accordingly, we first investigate the carbamate pathway. The non-bonded complexes, reactant complexes, transition states, and products involved in each pathway are designated as NB, RNB, TS, and P, respectively, and numbered according to the order of their appearance in the discussion.

3.2. Mechanism of the Carbamate Pathway. Several experimental and theoretical studies have demonstrated that the carbamate reaction pathway in amines proceeds via two steps where the zwitterion formation is the rate-determining step.[16,50−53] Table S17 shows the optimized geometries of the species involved in the carbamate pathway for pip and MP conformers: (MP + CO_2) non-bonded reactant complex (RNB1), TS1, and zwitterion (P1). In the first step (Table S17), RNB1 reacts to form a zwitterion (P1) for which the activation energy barriers were found to be quite low (<1 kcal/mol), while $\Delta^{\ddagger}G°$ values were slightly higher (∼1−3 kcal/mol). Among pip conformers in general, the COO^- group, being bulkier, tends to occupy the equatorial position. The highest energy barrier for the carbamate formation reaction was found for *trans*-eq 2-MP. Moreover, axial methyl groups tend to favor[27,49] the CO_2 approach in 2-MP as evident from the low E_a and $\Delta^{\ddagger}G°$ values associated with such conformers (especially for *trans*-ax 2-MP), resulting into a carbamate having an axial methyl and equatorially oriented COO^- group (Table S17). It can be concluded that most of the 3-MP and 4-MP conformers favor the carbamate pathway with an axial methyl and equatorial COO^- group (for the incoming CO_2) as the most preferred orientation with low energy barriers.

It is noteworthy that the TS1 and P1 were found to be stable only in the aqueous phase, while these species were not found to be at a saddle point and local minimum, respectively, in the gas phase. This peculiar behavior of TS1 and P1 zwitterionic species has also been observed in some previous studies.[16,55] Additionally, it has been demonstrated that the solvent (e.g., water) aids in lowering the activation energy for amine−CO_2 interactions by assisting the C−N bond formation.[21] This reinstates the importance of including solvent effects while modeling such interactions. From Table S17, it is observed that the C−N bond distance in TS1 of all piperidines varies from 2.26 to 2.58 Å, which decreases to 1.57−1.62 Å as P1 forms, while the O−C−O bond angle decreases to 133.4−134.6° in P1 (from 158.8 to 169.8° in TS1). The low E_a of the CO_2 + MP reaction suggests that this step is kinetically favored being thus a fast reaction. The energy profile of MPs obtained for zwitterion formation during the carbamate pathway is shown in Figure 2a (E_a = 0.75 kcal/mol), and the corresponding IRC curve thus obtained is given in Figure S4. Among various MP conformers, *cis*-ax 4-MP and *trans*-eq 4-MP are illustrated here, being the most stable conformers of 4-MP in the aqueous and gas phases.

For the gas phase (NB2 → RNB2 → TS2 → P2), a TS (TS2) for the proton transfer step is identified, which ultimately follows the carbamic acid pathway as indicated in the energy profile diagram (Figure 2b). However, this pathway proceeds with a higher energy barrier (12.43 kcal/mol). During this reaction, the MP−CO_2 interaction is assisted by a second MP molecule (Brønsted base), which is shown as RNB2 in Figure 2b. The TS2 leads to an intermediate (methylpiperidinium carbamate), which further forms the carbamic acid product (P2) via an intermolecular proton transfer.

The second step in the aqueous carbamate pathway involves an intermolecular proton transfer via another piperidine

https://doi.org/10.1021/acs.jpca.3c00406
J. Phys. Chem. A 2023, 127, 3123−3132

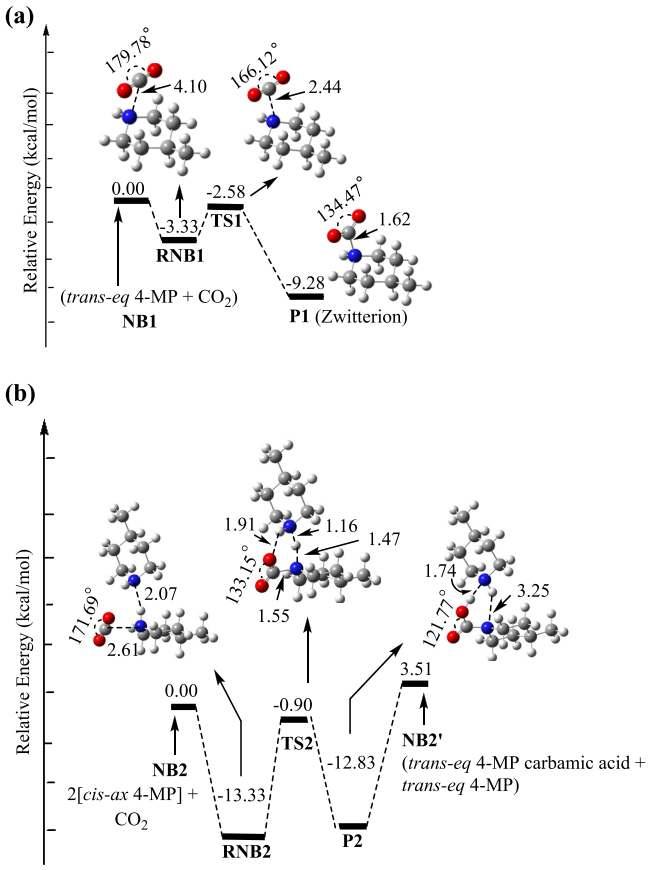

Figure 2. (a) Schematic illustration of the energy profile of the zwitterion formation (step 1 of the carbamate pathway) for aqueous *trans*-eq 4-MP; (b) 2:1 amine: CO_2 reaction of *cis*-ax 4-MP in the gas phase leading to the carbamic acid product and their corresponding B3LYP optimized structures. Bond angles (°), bond lengths (Å), and relative energies (kcal/mol) of each species are indicated.

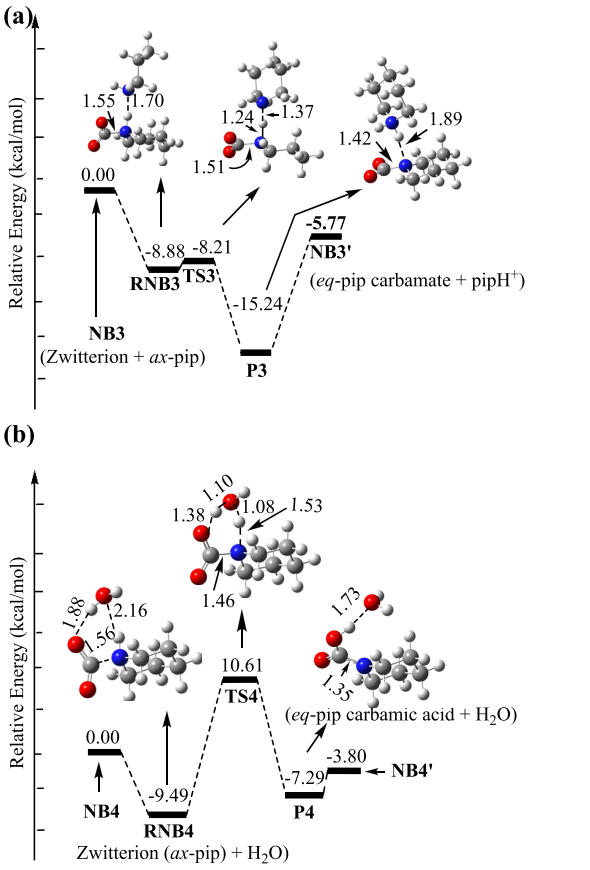

Figure 3. Schematic illustration of the energy profile of carbamate formation via (a) zwitterion−ax-pip interaction, (b) zwitterion−H_2O interaction for ax-pip, and the corresponding B3LYP-optimized structures (SMD model). Bond lengths (Å) and relative energies (kcal/mol) of the species are indicated.

molecule (acting as a Brønsted base), resulting in the carbamate product complex (P3). A PES scan corresponding to this step was performed in the aqueous phase with the H−N distance (H atom on the zwitterion and N atom of the second pip molecule) as the reaction coordinate. The TS could not be located for this step in the solvent phase, which indicates that proton transfer could be a barrierless process that is independent of the conformer, similar to some earlier known cases.[16,50] Interestingly, a TS (TS3) for the proton transfer step could be obtained only for ax-pip, which is illustrated in Figure 3a (corresponding IRC provided in Figure S4). The relative energy profile shows that the E_a for TS3 is 0.67 kcal/mol, which reinstates that the zwitterion···pip interaction during carbamate formation is favorable.

Xie et al.[16] have previously demonstrated that the proton transfer step during carbamate formation in MEA is an acid−base reaction owing to the activation of the N−H bond through zwitterion formation. This results in the fast kinetics for this step, especially in an aqueous solution where proton transfer is even faster. The shortening of the C−N bond distance from RNB3 (1.55 Å) to P3 (1.42 Å) also indicates the preference for this pathway. We also investigated the catalytic effect of water on the zwitterion for the proton transfer step during carbamate formation. Figure 3b shows the role of water for the proton abstraction from the zwitterion (ax-pip) where the reactant complex, TS, and products are indicated as RNB4, TS4, and P4, respectively. The energy barrier for this reaction is calculated to be quite high (20.10 kcal/mol) as compared to the zwitterion-pip proton abstraction pathway (almost barrierless). This agrees with the previous studies,[16,21,50] which reported that amines act as better Brønsted bases than water during the proton transfer process. The calculations also reveal that the carbamic acid product formed during water-aided proton transfer is energetically less favored compared to the zwitterion intermediate.

3.3. Mechanism of the Carbamate Hydrolysis. Many previous studies on amine-based CO_2 capture have established that the bicarbonate generated during the process originates from the hydrolysis of the ammonium carbamate.[4−8,14,15] However, more recent studies have demonstrated that carbamate hydrolysis is not the major contributor of bicarbonate species during amine−CO_2 interactions due to the high energy barrier associated with this reaction.[6,17,21,51] Furthermore, it has also been experimentally verified for few acyclic amines that bicarbonate formation starts only after the depletion of the carbamate in the reaction medium as protonated amines discourage bicarbonate formation.[21] Thus, in order to verify these findings, we have also investigated the hydrolysis of the MP carbamates and their various conformers.

Table S18 shows the species involved in the carbamate hydrolysis reaction, namely, the (MP carbamate + H_2O) reactant complex, TS, and (bicarbonate + amine) product complex. This reaction has been considered to be a concerted but asynchronous reaction as it proceeds with the concurrent

https://doi.org/10.1021/acs.jpca.3c00406
J. Phys. Chem. A 2023, 127, 3123−3132

breaking of the O−H bond of the water molecule, stretching of the carbamate C−N bond (as evident from the C−N bond distance data in Table S18), and nucleophilic attack of a water molecule on CO_2. The amine (4-MP) acts as a base and protonates to generate a OH^- ion (fast reaction) followed by the nucleophilic attack of the OH^- ion on the CO_2 carbon. The corresponding relative energy profile is shown in Figure 4a for

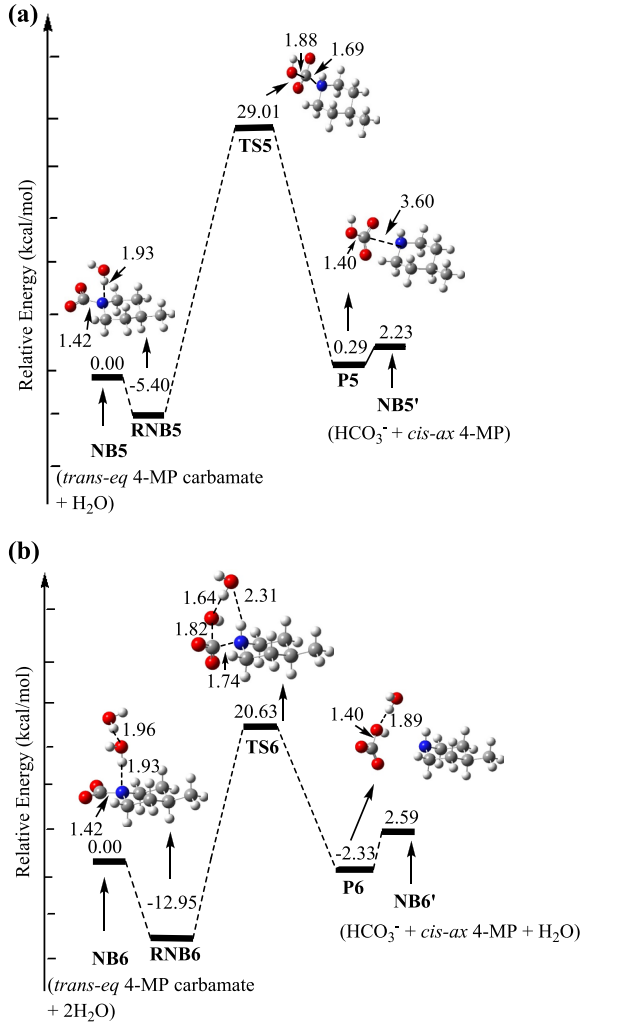

Figure 4. Schematic illustration of the energy profile of the hydrolysis reaction (Scheme 1) of *trans*-eq 4-MP carbamate utilizing (a) one molecule (b) and two molecules of water and the corresponding B3LYP-optimized structures obtained using SMD model. Bond lengths (Å) and relative energies (kcal/mol) of the species are indicated.

trans-eq 4-MP. The characteristic IRC curve (Figure S4) shows an initial small hump indicating the proton (from water) and N atom interaction followed by a steep curve for the nucleophilic attack of OH^- on CO_2 (E_a = 34.41 kcal/mol). Table S18 shows that the barrier for carbamate hydrolysis of MPs is quite high (E_a ≈ 33−37 and $\Delta^{\ddagger}G^{\circ}$ ≈ 34−38 kcal/mol) and thus seems implausible. Even after including two water molecules, the hydrolysis reaction indicates a high energy barrier (E_a ≈ 33 kcal/mol) as shown in Figure 4b. It is important to note that significant conformational changes are involved during product formation for both the carbamate reaction and its hydrolysis (Figures 2−4 and Tables S17 and S18). Thus, it is essential to explore the mechanistic parameters for each conformer of the MPs for the carbon capture reactions, rather than just considering the most stable conformer of each MP.

3.4. Mechanism of the Bicarbonate Pathway. The bicarbonate pathway involves the reaction of H_2O and CO_2 catalyzed by amine (pip) to form piperidinium bicarbonate. The optimized structures of the reactant complex, CO_2 + H_2O + MP (RNB7), TS (TS7) and product complex, and bicarbonate + protonated MP (P7) of all the MP conformers for this reaction in the aqueous phase are provided in Table S19. It is a single-step concerted reaction characterized by the abstraction of the proton from water by amine (pip/MP) followed by the nucleophilic attack of OH^- on CO_2. The computed E_a and $\Delta^{\ddagger}G^{\circ}$ values for piperidine and MP vary between 7.00 and 10.00 kcal/mol. The energy profile of the bicarbonate pathway for *trans*-eq 4-MP (E_a = 8.79 kcal/mol) is shown in Figure 5, and the relevant IRC curve (Figure S4) also corresponds to the desired set of reactant and products. Most of the hindered 2-MP conformers participate in the bicarbonate pathway, which is in contrast with their carbamate formation tendency. It can be proposed that the bicarbonate reaction pathway suits most of the MP conformers regardless of their structural geometry. Thus, it could be a predominant pathway for carbon capture in MPs along with the carbamate pathway, which is kinetically fast and suitable for unhindered primary and secondary amines.

Table 6 shows a comparative analysis of the energetic barriers and reaction free energies associated with CO_2 capture reactions in various acyclic and cyclic amines. It would be reasonable to compare the results from the present work with the previously obtained data at the B3LYP/6-311++G(d,p) level. Accordingly, the $\Delta^{\ddagger}G^{\circ}$ of the carbamate (zwitterion) formation reaction in case of MPs is quite comparable with acyclic amines such as MEA, methylamine, and EDA. All the results indicate a kinetically favored carbamate formation reaction. From Table 6, it is seen that similar calculations using CCSD(T) and MP2 levels of theory show significant variation in the results. The results of $\Delta^{\ddagger}G^{\circ}$ of the bicarbonate formation reaction show a high positive value for MEA and AMP, which could be compared with MPs even though the computation levels differ. Another interesting parameter is $\Delta\Delta G^{*}$, which is a straightforward indication of carbamate stability.[17] Accordingly, the carbamate formation tendency among acyclic and cyclic amines listed in the table should follow the order of MPs (B3LYP) > MEA > AMP > 2-PE (COSMO-RS//BP/TZVP), which reinstates the fast kinetics of the carbamate formation reaction in MPs. The ΔG_g and ΔG_{aq} values of MPs for carbamate hydrolysis reactions have already been discussed in the above sections, and these are quite comparable with other cyclic amines as observed in Table 6. Overall, the trends of activation energy barriers and reaction free energies of MPs computed at B3LYP-D3/SMD/6-311++G(d,p) agree reasonably well with the previously computed values (at different levels and solvation models) for various cyclic and acyclic amines. Thus, aqueous MPs should be explored further as potential post-combustion CO_2 capture solvents for large-scale industrial applications at par with other popular amine solvents, such as MEA.

4. CONCLUSIONS

This work explores various conformers of MPs for aqueous CO_2 capture reactions with the aid of appropriate thermodynamic models and the calculation of energy barriers for each capture pathway. Thermodynamic calculations pertaining to ΔG_{aq} and aqueous K_{eq} reveal that the energetically stable conformers of 3-MP and 4-MP show a facile carbamate formation tendency.

https://doi.org/10.1021/acs.jpca.3c00406
J. Phys. Chem. A 2023, 127, 3123−3132

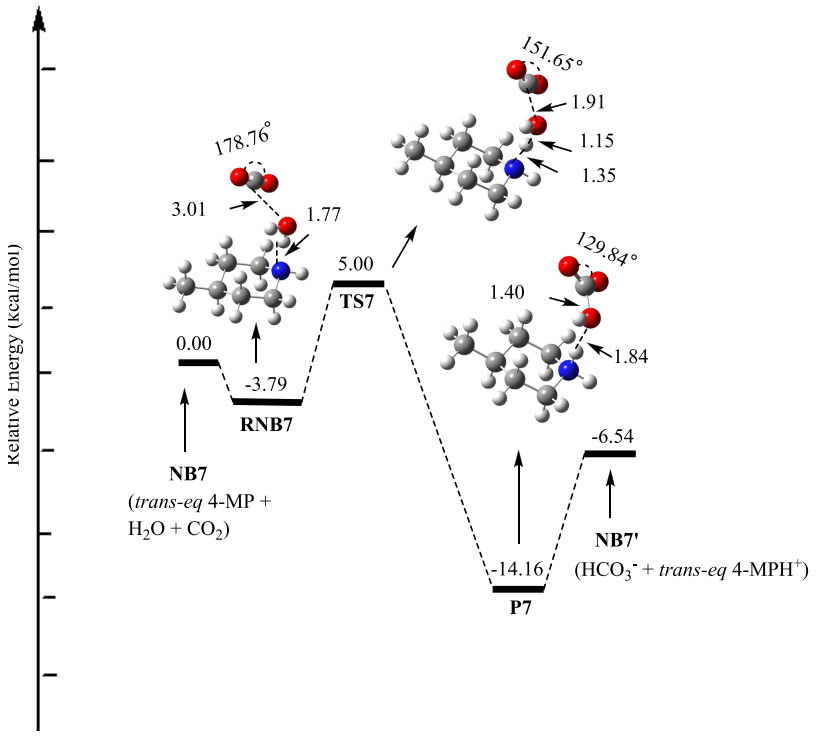

Figure 5. Schematic illustration of the energy profile of the bicarbonate reaction pathway (as seen in Scheme 1) of *trans*-eq 4-MP and the corresponding B3LYP-optimized structures obtained using the SMD model. Bond angles (°), bond lengths (Å), and relative energies (kcal/mol) are indicated.

Table 6. Comparison of Energetic Barriers and Other Mechanistic Parameters (kcal/mol) Involved in the CO_2 Capture Reactions in Various Acyclic and Cyclic Amines

	CO_2–amine reaction parameters				
amines	$\Delta^{\#}G^{\circ}$[e]	$\Delta^{\#}G^{\circ}$[f]	$\Delta\Delta G^{*}$[g]	ΔG_g[h]	ΔG_{aq}[i]
MEA[14,16,50,56]	4.1[a]* (12.0[b], 12.9[c])	18.0[c]	−4.2[d]	6.26[a]	−1.9[a]
CH_3NH_2[21]	2.4[a]*				
EDA[21]	5.2[a]*				
AMP[14,17,56]	17.8[c]	14.5[c]	−1.5[d]	1.13[a]	−8.8[a]**
morpholine[14]				2.3[a]	−3.7[a]**
piperazine[14]				0.5[a]	−4.8[a]**
2-PE[17]			0.3[d]		
MPs (this work)	1.0 to 3.0	∼8 to 10	−5.5 to −8.5	1.0 to −4.9	−3.7 to −10.8

[a]Computation at B3LYP/6-311++G(d,p); CPCM[a]*/PCM/IEFPCM[a]** model. [b]at CCSD(T)/6-311++G(d,p), CPCM model. [c]at SCS-MP2/6-311 + G(2d,2p), SMD model. [d]at COSMO-RS//BP/TZVP. [e]Activation free energy of the carbamate (zwitterion) formation reaction. [f]Activation free energy of the bicarbonate formation reaction. [g]Difference in activation free energies of carbamate and bicarbonate formation reactions. [h]Gas-phase reaction free energies of carbamate hydrolysis. [i]Solution phase reaction free energies of carbamate hydrolysis.

ΔG_{aq} values in general are exoergic for each capture pathway, while ΔG_g values are mostly endoergic during carbamate hydrolysis (which could be due to the inclusion of dispersion effects in the calculations). The activation free energies for the carbamate pathway (zwitterion formation) are quite lower (1−3 kcal/mol) than the values obtained excluding dispersion corrections. During the proton transfer step in the carbamate pathway, the zwitterion−amine route shows a much lower energy barrier than the zwitterion−H_2O route. For the carbamate hydrolysis reaction, even two explicit water molecules do not exhibit any significant effect on the high energy barrier.

Energetically stable hindered *trans*-eq 2-MP shows the least tendency toward carbamate reactions, while *cis*-eq 2-MP tends to follow the carbamate pathway with greater ease. Additionally, *trans*-ax 2-MP also shows preference for the carbamate pathway and this is in accordance with the previous experimental works based on IR and NMR data of the resulting carbamate.[27,49] Moreover, some of the other conformers of MPs such as the *cis*-ax 3-MP and *trans*-ax 4-MP also show low barrier heights for carbamate formation, which indicates that the axial methyl and equatorial COO^- group could be an energetically viable and ideal orientation of the functional groups in the carbamate product of MPs. Due to notable conformational variations involved in the carbamate formation and its hydrolysis, the mechanistic parameters of each possible conformers of MPs have been explored. Although carbamate formation can be achieved with greater ease, MP carbamate may be a minor product, especially for sterically hindered conformations. The bicarbonate pathway, which originates from the CO_2 + H_2O + MP reaction should be the predominant capture pathway yielding bicarbonate as the major product during carbon capture in aqueous MPs.

■ ASSOCIATED CONTENT

Supporting Information

The Supporting Information is available free of charge at https://pubs.acs.org/doi/10.1021/acs.jpca.3c00406.

Geometrical parameters of eq pip, optimized structure of eq- pip, rotational parameters of eq- and ax-pip, proton affinities (PAs), and gas phase basicities (GPBs) of MPs, methods to compute ΔG_{aq}, K_{eq}, BSSE-corrected ΔE_{int} and the results of ΔG_g, ΔG_{sol}, $\Delta\Delta G_{sol}$, K_{eq} data, ΔE_{int} for all

https://doi.org/10.1021/acs.jpca.3c00406
J. Phys. Chem. A 2023, 127, 3123−3132

MP conformers, optimized geometries of the conformers of 4-MP-CO_2 non-bonded complexes, geometrical parameters of the pip−CO_2 complex, optimized structure of the pip−CO_2 complex, optimized geometries, changes in the bond length and O−C−O bond angles, activation energies of the species involved in the capture reactions for each MP conformer, and characteristic IRC curves for each capture reaction (PDF)

Cartesian coordinates of the chemical species involved in the CO_2−MP reactions (PDF)

AUTHOR INFORMATION

Corresponding Authors

Uttama Mukherjee − *Department of Chemistry and Centre for Energy Science, Indian Institute of Science Education and Research, Pune 411008 Maharashtra, India;* orcid.org/0000-0003-4855-1875; Email: uttama.mukherjee@acads.iiserpune.ac.in

Prabhat Prakash − *Department of Chemistry and Centre for Energy Science, Indian Institute of Science Education and Research, Pune 411008 Maharashtra, India; Chemistry and Chemical Engineering, MC 139-74, California Institute of Technology, Pasadena, California 91125, United States;* orcid.org/0000-0003-1430-2379; Email: prabhat.prakash@students.iiserpune.ac.in

Arun Venkatnathan − *Department of Chemistry and Centre for Energy Science, Indian Institute of Science Education and Research, Pune 411008 Maharashtra, India;* orcid.org/0000-0001-8450-5417; Phone: +91-20-2590-8085; Email: arun@iiserpune.ac.in; Fax: +91-20-2586-5315

Complete contact information is available at: https://pubs.acs.org/10.1021/acs.jpca.3c00406

Notes

The authors declare no competing financial interest.

ACKNOWLEDGMENTS

The authors acknowledge the National Supercomputing Mission (NSM) 'PARAM Brahma' at IISER Pune, which is implemented by C-DAC and supported by the Ministry of Electronics and Information Technology (MeitY) and Department of Science and Technology (DST), Government of India. U.M. acknowledges DST for providing the WOS-A fellowship, grant no. SR/WOS-A/CS-3/2020.

REFERENCES

(1) Hasan, S.; Abbas, A. J.; Nasr, G. G. Improving the Carbon Capture Efficiency for Gas Power Plants through Amine-Based Absorbents. *Sustainability* **2021**, *13*, 72.

(2) Crooks, J. E.; Donnellan, J. P. Kinetics and Mechanism of the Reaction between Carbon Dioxide and Amines in Aqueous Solution. *J. Chem. Soc., Perkin Trans. 2* **1989**, *2*, 331−333.

(3) Versteeg, G. F.; van Dijck, L. A. J.; van Swaaij, W. P. M. On the kinetics between CO_2 and alkanolamines both in aqueous and nonaqueous solutions. An overview. *Chem. Eng. Commun.* **1996**, *144*, 113−158.

(4) Yoon, S. J.; Lee, H. Substituent Effect in Amine-CO_2 interaction investigated by NMR and IR Spectroscopies. *Chem. Lett.* **2003**, *32*, 344−345.

(5) Arstad, B.; Blom, R.; Swang, O. CO_2 Absorption in Aqueous Solutions of Alkanolamines: Mechanistic Insight from Quantum Chemical Calculations. *J. Phys. Chem. A* **2007**, *111*, 1222−1228.

(6) Kortunov, P. V.; Siskin, M.; Baugh, L. S.; Calabro, D. C. In Situ Nuclear Magnetic Resonance Mechanistic Studies of Carbon Dioxide Reactions with Liquid Amines in Aqueous Systems: New Insights on Carbon Capture Reaction Pathways. *Energy Fuels* **2015**, *29*, 5919−5939.

(7) Kortunov, P. V.; Siskin, M.; Paccagnini, M.; Thomann, H. CO_2 Reaction Mechanisms with Hindered Alkanolamines: Control and Promotion of Reaction Pathways. *Energy Fuels* **2016**, *30*, 1223−1236.

(8) Yu, J.; Chuang, S. S. C. The Role of Water in CO_2 Capture by Amine. *Ind. Eng. Chem. Res.* **2017**, *56*, 6337−6347.

(9) da Silva, E. F.; Svendsen, H. F. Computational chemistry study of reactions, equilibrium and kinetics of chemical CO_2 absorption. *Int. J. Greenhouse Gas Control* **2007**, *1*, 151−157.

(10) Bonenfant, D.; Mimeault, M.; Hausler, R. Determination of the Structural Features of Distinct Amines Important for the Absorption of CO_2 and Regeneration in Aqueous Solution. *Ind. Eng. Chem. Res.* **2003**, *42*, 3179−3184.

(11) Vaidya, P. D.; Kenig, E. Y. CO_2-Alkanolamine Reaction Kinetics: A Review of Recent Studies. *Chem. Eng. Technol.* **2007**, *30*, 1467−1474.

(12) Sartori, G.; Savage, D. W. Sterically Hindered Amines for Carbon dioxide Removal from Gases. *Ind. Eng. Chem. Fundam.* **1983**, *22*, 239−249.

(13) Hook, R. J. An Investigation of Some Sterically Hindered Amines as Potential Carbon Dioxide Scrubbing Compounds. *Ind. Eng. Chem. Res.* **1997**, *36*, 1779−1790.

(14) da Silva, E. F.; Svendsen, H. F. Study of the Carbamate Stability of Amines Using ab Initio Methods and Free-Energy Perturbations. *Ind. Eng. Chem. Res.* **2006**, *45*, 2497−2504.

(15) Jackson, P.; Beste, A.; Attalla, M. Insights into amine-based CO_2 capture: an ab initio self-consistent reaction field investigation. *Struct. Chem.* **2011**, *22*, 537−549.

(16) Xie, H.-B.; Zhou, Y.; Zhang, Y.; Johnson, J. K. Reaction Mechanism of Monoethanolamine with CO_2 in Aqueous Solution from Molecular Modeling. *J. Phys. Chem. A* **2010**, *114*, 11844−11852.

(17) Yamada, H.; Matsuzaki, Y.; Okabe, H.; Shimizu, S.; Fujioka, Y. Quantum Chemical Analysis of Carbon dioxide Absorption into Solutions of Moderately Hindered Amines. *Energy Procedia* **2011**, *4*, 133−139.

(18) Stowe, H. M.; Vilciauskas, L.; Paek, E.; Hwang, G. S. On the Origin of Preferred Bicarbonate Production from Carbon dioxide (CO_2) Capture in Aqueous 2-amino-2-methyl-1-propanol (AMP). *Phys. Chem. Chem. Phys.* **2015**, *17*, 29184−29192.

(19) Svensson, H.; Edfeldt, J.; Velasco, V. Z.; Hulteberg, C.; Karlsson, H. T. Solubility of carbon dioxide in mixtures of 2-amino-2-methyl-1-propanol and organic solvents. *Int. J. Greenhouse Gas Control* **2014**, *27*, 247−254.

(20) Yamada, H. Comparison of Solvation Effects on CO_2 Capture with Aqueous Amine Solutions and Amine-Functionalized Ionic Liquids. *J. Phys. Chem. B* **2016**, *120*, 10563−10568.

(21) Said, R. B.; Kolle, J. M.; Essalah, K.; Tangour, B.; Sayari, A. A Unified Approach to CO_2−Amine Reaction Mechanisms. *ACS Omega* **2020**, *5*, 26125−26133.

(22) García-Abuín, A.; Gómez-Díaz, D.; Navaza, J. M.; Vidal-Tato, I. Kinetics of carbon dioxide chemical absorption into cyclic amines solutions. *AIChE J.* **2011**, *57*, 2244−2250.

(23) García-Abuín, A.; Gómez-Díaz, D.; Navaza, J. M.; Rumbo, A. CO_2 Capture by Pyrrolidine: Reaction Mechanism and Mass Transfer. *AIChE J.* **2014**, *60*, 1098−1106.

(24) Robinson, K.; McCluskey, A.; Attalla, M. I. An FTIR Spectroscopic Study on the Effect of Molecular Structural Variations on the CO_2 Absorption Characteristics of Heterocyclic Amines. *ChemPhysChem* **2011**, *12*, 1088−1099.

(25) Castro, M.; Gómez-Díaz, D.; Navaza, J. M. Carbon dioxide Chemical Absorption Using Methylpiperidines Aqueous Solutions. *Fuel* **2017**, *197*, 194−200.

(26) Park, D. J.; Choi, J. H.; Kim, Y. E.; Nam, S. C.; Lee, K. B.; Yoon, Y. I. Chemical Absorption of Carbon dioxide Using Aqueous Piperidine Derivatives. *Chem. Eng. Technol.* **2017**, *40*, 2266−2273.

(27) McGregor, C.; Al-Abdul-Wahid, M. S.; Robertson, V.; Cox, J. S.; Tremaine, P. R. Formation Constants and Conformational Analysis of Carbamates in Aqueous Solutions of 2-Methylpiperidine and CO_2 from 283 to 313 K by NMR Spectroscopy. *J Phys Chem B* **2018**, *122*, 9178−9190.
(28) Coulier, Y.; Ballerat-Busserolles, K.; Rodier, L.; Coxam, J.-Y. Temperatures of Liquid−Liquid Separation and Excess Molar Volumes of {N-Methylpiperidine−Water} and {2-Methylpiperidine−Water} Systems. *Fluid Phase Equilib.* **2010**, *296*, 206−212.
(29) Choi, J. H.; Oh, S. G.; Jo, M.; Yoon, Y. I.; Jeong, S. K.; Nam, S. C. Absorption of Carbon Dioxide by the Mixed Aqueous Absorbents Using 2-Methylpiperidine as a Promoter. *Chem. Eng. Sci.* **2012**, *72*, 87−93.
(30) Sherman, B. J.; Ciftja, A. F.; Rochelle, G. T. Thermodynamic and mass transfer modeling of carbon dioxide absorption in to aqueous 2-piperidineethanol. *Chem. Eng. Sci.* **2016**, *153*, 295−307.
(31) Du, Y.; Wang, Y.; Rochelle, G. T. Piperazine/4-hydroxy-1-methylpiperidine for CO_2 capture. *Chem. Eng. J.* **2017**, *307*, 258−263.
(32) Dubois, L.; Thomas, D. Screening of Aqueous Amine-Based Solvents for Postcombustion CO_2 Capture by Chemical Absorption. *Chem. Eng. Technol.* **2012**, *35*, 513−524.
(33) Frisch, M. J.; Trucks, G. W.; Schlegel, H. B.; Scuseria, G. E.; Robb, M. A.; Cheeseman, J. R.; Scalmani, G.; Barone, V.; Mennucci, B.; Petersson, G. A., et al. *Gaussian 09, Revision D.01*; Gaussian, Inc., Wallingford CT. 2010.
(34) Becke, A. D. Density-functional thermochemistry. IV. A new dynamical correlation functional and implications for exact-exchange mixing. *J. Chem. Phys.* **1996**, *104*, 1040−1046.
(35) Zhao, Y.; Truhlar, D. G. The M06 Suite of Density Functionals for Main Group Thermochemistry, Thermochemical Kinetics, Noncovalent Interactions, Excited States, and Transition Elements: Two New Functionals and Systematic Testing of Four M06-Class Functionals and 12 Other Functionals. *Theor. Chem. Acc.* **2008**, *120*, 215−241.
(36) Grimme, S.; Antony, J.; Ehrlich, S.; Krieg, H. A Consistent and Accurate Ab Initio Parametrization of Density Functional Dispersion Correction (DFT-D) for the 94 Elements H-Pu. *J. Chem. Phys.* **2010**, *132*, 154104−154123.
(37) Kolaski, M.; Kumar, A.; Singh, N. J.; Kim, K. S. Differences in Structure, Energy, and Spectrum between Neutral, Protonated, and Deprotonated Phenol Dimers: Comparison of Various Density Functionals with ab initio Theory. *Phys. Chem. Chem. Phys.* **2011**, *13*, 991−1001.
(38) Marenich, A. V.; Cramer, C. J.; Truhlar, D. G. Universal Solvation Model Based on Solute Electron Density and on a Continuum Model of the Solvent Defined by the Bulk Dielectric Constant and Atomic Surface Tensions. *J. Phys. Chem. B* **2009**, *113*, 6378−6396.
(39) Cramer, C. J.; Truhlar, D. G. Implicit Solvation Models: Equilibria, Structure, Spectra, and Dynamics. *Chem. Rev.* **1999**, *99*, 2161−2200.
(40) Peng, C.; Bernhard Schlegel, H. Combining Synchronous Transit and Quasi-Newton Methods to Find Transition States. *Isr. J. Chem.* **1993**, *33*, 449−454.
(41) Fukui, K. The Path of Chemical Reactions-The IRC Approach. *Acc. Chem. Res.* **1981**, *14*, 363−368.
(42) Hratchian, H. P.; Schlegel, H. B. Accurate Reaction Paths Using a Hessian Based Predictor-Corrector Integrator. *J. Chem. Phys.* **2004**, *120*, 9918−9924.
(43) Raczyńska, E. D.; Makowski, M.; Górnicka, E.; Darowska, M. Ab Initio Studies on the Preferred Site of Protonation in Cytisine in the Gas Phase and Water. *Int. J. Mol. Sci.* **2005**, *6*, 143−156.
(44) Bryantsev, V. S.; Diallo, M. S.; Goddard, W. A., III Calculation of Solvation Free Energies of Charged Solutes Using Mixed Cluster/Continuum Models. *J. Phys. Chem. B* **2008**, *112*, 9709−9719.
(45) Chipman, D. M. Anion Electric Field is Related to Hydration Energy. *J. Chem. Phys.* **2003**, *118*, 9937.
(46) Chipman, D. M.; Chen, F. Cation electric field is related to hydration energy. *J. Chem. Phys.* **2006**, *124*, 144507.
(47) Lee, H. M.; Youn, I. S.; Saleh, M.; Lee, J. W.; Kim, K. S. Interactions of CO_2 with Various Functional Molecules. *Phys. Chem. Chem. Phys.* **2015**, *17*, 10925−10933.
(48) Jiang, H.; Zhang, S.; Xu, Y. Molecular Complex Piperidine-CO_2. *Afr. J. Pure Appl. Chem.* **2009**, *3*, 126−130.
(49) Fandino, O.; Sasidharanpillai, S.; Soldatov, D. V.; Tremaine, P. R. Carbamate Formation in the System (2-Methylpiperidine + Carbon Dioxide) by Raman Spectroscopy and X-ray Diffraction. *J. Phys. Chem. B* **2018**, *122*, 10880−10893.
(50) Shim, J.-G.; Kim, J.-H.; Jhon, Y. H.; Kim, J.; Cho, K.-H. DFT Calculations on the Role of Base in the Reaction between CO_2 and Monoethanolamine. *Ind. Eng. Chem. Res.* **2009**, *48*, 2172−2178.
(51) Matsuzaki, Y.; Yamada, H.; Chowdhury, F. A.; Higashii, T.; Onoda, M. Ab Initio Study of CO_2 Capture Mechanisms in Aqueous Monoethanolamine: Reaction Pathways for the Direct Interconversion of Carbamate and Bicarbonate. *J. Phys. Chem. A* **2013**, *117*, 9274−9281.
(52) Cho, M.; Park, J.; Yavuz, C. T.; Jung, Y. A Catalytic Role of Surface Silanol Groups in CO_2 Capture on the Amine-Anchored Silica Support. *Phys. Chem. Chem. Phys.* **2018**, *20*, 12149−12156.
(53) Li, K.; Kress, J. D.; Mebane, D. S. The Mechanism of CO_2 Adsorption under Dry and Humid Conditions in Mesoporous Silica-Supported Amine Sorbents. *J. Phys. Chem. C* **2016**, *120*, 23683−23691.
(54) Lonsdale, R.; Harvey, J. N.; Mulholland, A. J. Effects of Dispersion in Density Functional Based Quantum Mechanical/Molecular Mechanical Calculations on Cytochrome P450 Catalyzed Reactions. *J. Chem. Theory Comput.* **2012**, *8*, 4637−4645.
(55) da Silva, E. F.; Svendsen, H. F. Ab Initio Study of the Reaction of Carbamate Formation from CO_2 and Alkanolamines. *Ind. Eng. Chem. Res.* **2004**, *43*, 3413−3418.
(56) Gangarapu, S.; Marcelis, A. T. M.; Alhamed, Y. A.; Zuilhof, H. The Transition States for CO_2 Capture by Substituted Ethanolamines. *Chem. Phys. Chem.* **2015**, *16*, 3000−3006.

https://doi.org/10.1021/acs.jpca.3c00406
J. Phys. Chem. A 2023, 127, 3123−3132